

Mining Objects: Fully Unsupervised Object Discovery and Localization From a Single Image

Runsheng Zhang, Yaping Huang, Mengyang Pu, Jian Zhang, Qingji Guan, Qi Zou, Haibin Ling *Member, IEEE*,

Abstract—The goal of our work is to discover dominant objects without using any annotations. We focus on performing unsupervised object discovery and localization in a very general setting where only a single image is given. This is far more challenge than typical co-localization or weakly-supervised localization tasks. To tackle this problem, we propose a simple but effective pattern mining-based method, called Object Location Mining (OLM), which exploits the advantages of data mining and feature representation of pre-trained convolutional neural networks (CNNs). Specifically, we first convert the feature maps from a pre-trained CNN model into a set of transactions, and then discovers frequent patterns from transaction database through pattern mining techniques. We observe that those discovered patterns, *i.e.*, co-occurrence highlighted regions, typically hold appearance and spatial consistency. Motivated by this observation, we can easily discover and localize possible objects by merging relevant meaningful patterns in an unsupervised manner. Extensive experiments on eleven benchmarks demonstrate that OLM achieves competitive localization performance compared with the state-of-the-art methods. We also evaluate our approach compared with unsupervised saliency detection methods and achieves best results on four benchmark datasets. Moreover, we conduct experiments on fine-grained classification to show that our proposed method can locate the entire object and parts accurately, which can benefit to improving the classification results significantly.

Index Terms—unsupervised object discovery, pattern mining, convolutional neural networks

I. INTRODUCTION

OBJECT discovery and localization is a fundamental computer vision problem, and it aims to discover and locate interesting objects within an image. Benefiting from the learning capability of deep convolutional neural networks and large-scale object bounding box annotations, object localization has achieved remarkable performance [1], [2]. However, it is expensive and labor-intensive to manually annotate bounding boxes on the large-scale dataset. This motivates the development of weakly supervised object localization methods, which only use image-level annotations to localize objects. Most existing weakly supervised object localization methods locate the objects by training a classification convolutional neural network with image-level annotations [3], [4], [5]. Recently, some works [6], [7], [8], [9], [10] shift their attention to image co-localization problem, which assumes less supervision and requires a set of images containing objects from a common category. But most of these efforts usually need to first

R. Zhang, Y. Huang, Q. Zou, M. Pu, J. Zhang and Q. Guan are with the Beijing Key Laboratory of Traffic Data Analysis and Mining, Beijing Jiaotong University, Beijing 100044, China (e-mail: rszhang, yphuang, mengyangpu, jianzhang1, qzou@bjtu.edu.cn, qingjiguan@gmail.com).

H. Ling is with the Department of Computer Sciences, Stony Brook University, Stony Brook, NY 11794-2424 USA (e-mail: hling@cs.stonybrook.edu).

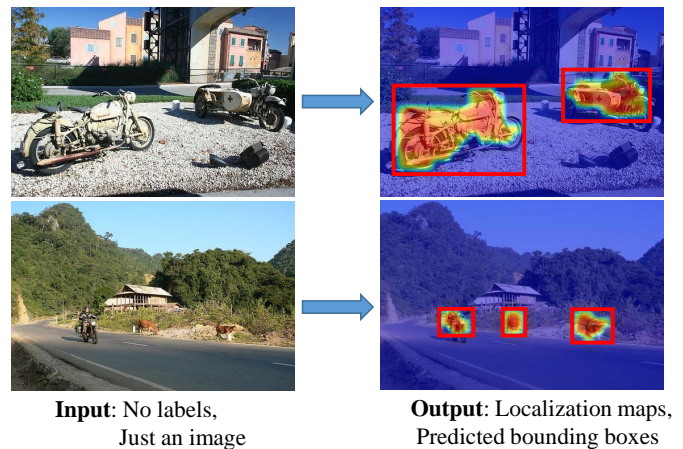


Fig. 1. Fully unsupervised object localization from a single image. We tackle this problem in a challenging setting where only an image is given, without any type of annotations or even a set of images containing objects from the same category. Our proposed method discovers dominant object instances (red bounding boxes) based on their localization maps. (Best viewed in color.)

generate enormous object proposals. This may lead to high time consumption and the performance heavily depends on the quality of the proposals.

In this paper, we address unsupervised object localization in a far more challenging and more realistic scenario where only a single image is given. As illustrated in Figure 1, the setting of our method is fully unsupervised, without utilizing any annotations or even a single dominant class. In fact, unsupervised localization is an extremely common problem due to the fact that most images in real life are usually with unknown categories or even without labels. Therefore, it is worth developing object localization methods from unlabeled images.

Recent works [11], [12], [3] demonstrate that the pre-trained CNN models could provide powerful semantic representation for a given image. This raises a natural question that “Is it possible to obtain localization maps without training or fine-tuning by mining the generic localization ability of pre-trained models?”

Previous works [3], [13] have revealed that the convolutional activations usually fire at the same region that may be a general part of an object. [13] employs a simple “mean-threshold” strategy to localize the objects. They add up the *Pool-5* activation tensor through the depth direction and calculate the mean value as the threshold to decide which positions belong to objects. However, such simple strategy is only evaluated on fine-grained datasets. In fact, the key weakness

of the localization maps generated by [13] is that even if the activation responses of one region are higher than the mean value in only one single channel, the regions will also be fired, which leads to the localization results are not very robust to the noisy background on complex images. Therefore, it is of great interest to develop more efficient approaches to automatically discover and utilize these co-occurrence visual patterns, which would be beneficial to identify integral object regions.

To tackle the above issues, this paper proposes a novel and simple approach, named Object Location Mining (OLM), to mine frequent patterns and discover objects from the pattern mining perspective. The success of our proposed method relies on two key foundations: 1) The CNN features extracted from the pre-trained model have powerful representation and provide abundant semantic and spatial information; 2) Pattern mining techniques can efficiently mine frequently-occurring visual patterns, which often indicate the location of objects in one image.

Our proposed OLM first converts the deep features from the particular layer of a pre-trained CNN model into a set of transactions (*i.e.* a transaction database). Specifically, we propose an efficient transaction creation strategy: we extract the deep features from multiple convolutional layers and use a tunable threshold to select the descriptors that are used to convert to items. Benefiting from this strategy, we could retain the most useful information while discarding redundant information, which is critical to obtain a suitable input for a mining algorithm. Then we look for relevant but non-redundant patterns automatically through pattern mining techniques. Finally, we merge the selected patterns to generate a support map which represents the object regions. The experimental results show that the discovered regions are not only semantically consistent but also accurately cover the objects. Based on the mined objects, it allows for a more efficient part localization and can be easily integrated with fine-grained classification models.

Our proposed method is simple but effective, which does not need the training process. Thus, we do not need to design complex loss function and avoid collecting a large amount of annotations which is labor consuming. More importantly, compared with co-localization methods, we address unsupervised object localization in more challenging scenarios where only a single image is given. It is more reasonable in the practical scenario.

To the best of our knowledge, we propose the first usage of pattern mining for fully-unsupervised object localization. The main contributions are summarized as follows:

- We propose an effective unsupervised object discovery and localization method based on pattern mining techniques, named Object Location Mining (OLM), which is fully unsupervised and does not need the training or fine-tuning process.
- We propose an efficient transaction creation strategy to transform the convolutional activations into transactions, which is the key issue for the success of pattern mining techniques.
- Extensive experiments are conducted on eleven datasets include four fine-grained datasets, Object Discovery

dataset, ImageNet subsets and PASCAL VOC 2007 dataset. Our proposed method outperforms other fully-unsupervised methods by a large margin. Moreover, we also evaluate the localization ability on unsupervised saliency detection and fine-grained classification task. Our method achieves competitive performance compared with the state-of-the-art methods.

II. RELATED WORK

In this section, we review related works on unsupervised object discovery, and its extension to fine-grained image classification and saliency detection, and the strategies of the pattern mining which inspire us a novel solution to the proposed method.

A. Unsupervised Object Localization

Fully unsupervised localization is challenging due to the fact that it does not depend on any auxiliary information rather than a given image. Thus, many methods shift their attention to solve image co-localization problem [14], [15], [7], [6], [8], [9], [10].

The key difference is that image co-localization requires a set of images containing objects from the same category whereas fully unsupervised localization deals with only one single image. Some earlier image co-localization methods [14], [15], [7], [8] address this problem based on low-level features (*e.g.*, SIFT, HOG). [9] is the first to use the features from fully connected layer of a pre-trained CNN model to learn a common object detector. However, the spatial correlation of deep descriptors in convolutional layers are lost. [16], [3] demonstrate that the convolutional activations remain spatial and semantic information and have remarkable localization ability. [10] utilizes the convolutional activations and further considers their correlations in an image collection to deal with image co-localization problem.

Since fully unsupervised image localization is a very challenging problem, there exist a limited number of comparable methods such as [13]. [13] extracts feature descriptors from the last max-pooling layer of a pre-trained VGG-16 model [17] and employs a simple “mean-threshold” strategy to locate the main objects in fine-grained images. Compared with [13], our pattern mining-based method considers a more reasonable and more general measurement only those areas that are frequently activated in many channels will be fired. Thus, our method is more robust to the noisy background and can mine more distinctive object regions.

B. Fine-grained Image Classification

Fine-grained image classification is one of the most fundamental and important task in computer vision, and a large amount of works have been developed in the past few years. Benefited from the advancement of deep learning, many works [18], [17], [19], [20], [21] learn more discriminative feature representation by leveraging deep CNNs, and achieve significant progress.

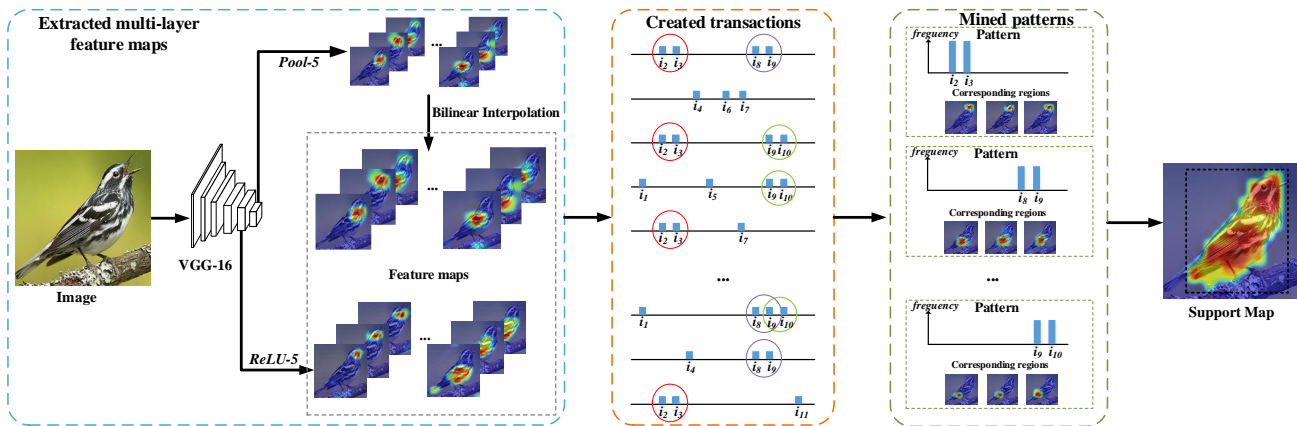


Fig. 2. Overview of our proposed OM for unsupervised object localization. First, feature maps (*Pool-5* layer and *ReLU-5* layer) are extracted from a VGG-16 model [17] pre-trained on ImageNet, and feature maps from *Pool-5* layer are resized to the same size of *ReLU-5* layer by bilinear interpolation. Then, we transform those feature maps into a transaction database, thus meaningful patterns could be discovered from the transaction database through Object Mining. Finally, a support map is generated by merging the meaningful patterns.

Since subtle visual differences mostly reside in local regions of parts, discriminative part localization is crucial for fine-grained image classification. There are numerous emerging works proceeding along part localization. [19], [22], [23], [24] learn accurate part localization models with manual object bounding boxes and part annotations. Considering that the annotations are laborious and expensive, some works [25], [26], [27], [20], [28], [29], [30], [31] instead focus on how to exploit parts under a weakly-supervised setting with only image-level labels. [26] proposes an automatic fine-grained classification method, incorporating deep convolutional filters with significant and consistent responses for both parts selection and representation. Some of the above part localization-based methods [25], [20], [26], [32] usually require to firstly produce object or part candidates by selective search [33], which poses challenges to accurate part localization.

Additionally, some weakly-supervised methods [34], [20], [28], [29], [30], [31] use visual attention mechanism to automatically capture the informative regions. [29] employs a fully convolutional attention network to adaptively localize multiple parts simultaneously. Recent works [30], [31] propose an end-to-end framework where part localization and feature learning mutually reinforce each other. Although promising results have been reported, it is highly difficult to train the models due to sophisticated alternative training procedures.

Since part localization is a key issue in fine-grained classification, it is natural to extend our Object Mining method to part localization. Therefore, we further propose an efficient part localization method. Our method does not need sophisticated training procedures. We can directly localize multiple fine-grained parts instead of selecting useful ones from enormous part proposals with high cost [35].

C. Saliency detection

Saliency detection aims to automatically discover and locate the most salient regions in an image that draw human attention. Depending on annotations used, saliency detection methods can be roughly divided into two categories: unsupervised

methods and supervised methods. [36] and [37] provide the detailed reviews of saliency detection. Our work focuses on unsupervised solution and thus is more related to unsupervised saliency detection methods, which mainly rely on different priors. For example, Hierarchical Saliency (HS) [38] attempts to utilize the global contrast prior to distinguish the salient objects. MC [39] separates salient objects from the background via absorbing Markov chain. DRFI [40] integrates the regional contrast, regional property and regional backgroundness descriptors together to produce the saliency map. DSR [41] extracts image boundaries via superpixels and then constructs dense and sparse appearance models.

More recently, CNN models are gradually becoming the mainstream solution in saliency detection. These approaches can achieve state-of-the-art performance due to the encoding of high-level semantic features. However, the CNN-based methods strongly require large-scale annotated training data, which are not only labor-intensive but also computation expensive. Some methods explore a combination of deep learning and the unsupervised setting to solve the problem of saliency detection. [42], [43] use existing unsupervised salient models to generate pseudo ground-truth, and then train a CNN-based model to solve the problem. Compared to the aforementioned methods, our method does not need any training process, leading to a more practical solution.

D. Pattern Mining in Computer Vision

Pattern mining techniques have been developed for several decades in the data mining community. Usually, a set of patterns is a combination of several elements and the distinctive information is captured. Inspired by this fact, many researchers investigate the problem of employing pattern mining to address computer vision tasks, including image classification [44], [45], image collection summarization [46] and object retrieval [45].

A key issue in pattern mining methods is how to transform an image into transaction data, which are suitable for pattern mining and maintain most of the corresponding discriminative

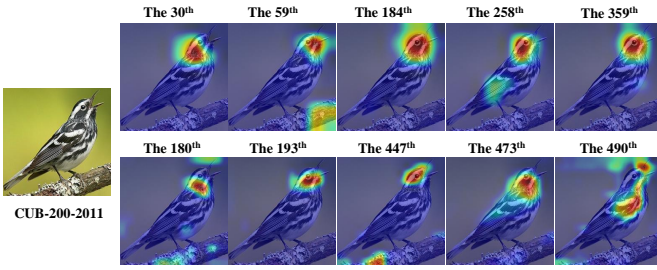


Fig. 3. Sampled feature maps of an image from CUB-200-2011 dataset. The first column is the input image, and the rest five feature maps of the first row are selected from *Pool-5*, and the five feature maps of the second row are select from *ReLU-5*. (Best viewed in color.)

information. Most early methods simply treat an individual visual word as an item in a transaction. Due to the sparsity of local bag-of-words (LBOW), LBOW is usually adopted as image representations in [47], [48], [49], then each visual word is treated as an item. However, this operation only considers the absence/presence of the visual word and may lead to information loss during transaction creation. To avoid the above issues, [50] proposes a frequent local histogram method to represent an image with the histograms of patterns sets. More recently, [44] is first to illustrate how pattern mining techniques are combined with the CNN features, a more appealing alternative than the hand-crafted features. In [44], a local patch is transformed into a transaction by treating each dimension index of a CNN activation as an item. However, it may suffers from the loss of the critical spatial information due to the features extracted from the fully connected layer.

III. THE PROPOSED METHOD

In this section, we provide details of our OLM approach. The overview of the proposed method is illustrated in Figure 2. First, we extract the feature maps from the *Pool-5* and *ReLU-5* layers of a pre-trained VGG-16 model. Then, the feature maps are converted into a set of transactions and the meaningful patterns are discovered by pattern mining techniques. Finally, we illustrate the details of how to merge the selected patterns to localize potential target regions.

A. Notations and terminology

First, we introduce the data mining notations and terminology. Let $I = \{i_1, i_2, \dots, i_M\}$ denote an itemset containing M items. A transaction $T \subseteq I$ satisfies $|T| \leq M$, where $|T|$ is the number of items in transaction T . We define a transaction database $D = \{T_1, T_2, \dots, T_N\}$. Given an itemset $P \subseteq I$, we calculate the frequency K of the itemset P in the transaction database D by $K = |\{T | T \in D, P \subseteq T\}|$. Then, we define the *support* value of P as:

$$\text{supp}(P) = \frac{K}{N} = \frac{|\{T | T \in D, P \subseteq T\}|}{N} \in [0, 1], \quad (1)$$

where $|\cdot|$ measures the cardinality, and N is the number of transactions in D . The itemset P whose *support* value is larger than a predefined threshold is considered as the *frequent itemset*. The itemset P is the pattern we want to mine.

B. Extracting multi-layer feature maps

Recent works demonstrate that different convolutional layers learn different level features [11]. Specifically, the deeper the convolutional layer, the better discriminative power it has. Thus, the general rule is that deeper convolutional layers are preferred to choose. In our work, the images are passed through a pre-trained VGG-16 [17] model and the feature maps are obtained from *Pool-5* and *ReLU-5* layers. This strategy allows us to take original images with arbitrary sizes as input, and also alleviates the loss of useful information caused by only considering single layer activations.

We randomly select an image from the fine-grained dataset (CUB-200-2011 [51]) and visualize the local response regions of *Pool-5* and *ReLU-5* layers. As shown in Figure 3, we can clearly observe that although the heatmaps of *Pool-5* and *ReLU-5* are not the same, most semantic parts of a bird are frequently activated at the same location in many feature channels. Moreover, these two layers can preserve more co-occurrence meaningful regions, which may be the corresponding parts of an object. However, some background regions are also activated. Fortunately, these regions only present in few channels and are distributed sparsely. That means not all activated areas in the feature maps are useful, so it is necessary to further mine the meaningful regions using pattern mining techniques.

C. From feature maps to transactions

It is the most critical step to convert data into a set of transactions while maintaining useful information when applying pattern mining techniques to computer vision applications. In our method, each feature map is treated as a transaction denoted by T , and each position index activated from the feature map is considered as an item i . For example, if there are five positions fired in the j -th feature map, the corresponding transaction T_j would include five items, *i.e.* $T_j = \{i_1, i_2, i_3, i_4, i_5\}$. The index set of all activated positions from all feature maps, also known as an itemset, is denoted by $I = \{i_1, i_2, \dots, i_m\}$. Each transaction is a subset of items I , *i.e.* $T \subseteq I$. The set of all transactions (*i.e.* all feature maps) is denoted by D . In our scenario, N feature maps correspond to N transactions, *i.e.* $D = \{T_1, T_2, \dots, T_N\}$.

In practice, an image with size $H \times W \times 3$ is fed into a pre-trained VGG-16 model [17]. Then we obtain 512 feature maps with size $\frac{H}{32} \times \frac{W}{32}$ from *Pool-5* and 512 feature maps with size $\frac{H}{16} \times \frac{W}{16}$ from *ReLU-5* respectively. We resize *Pool-5* feature maps to the same size with *ReLU-5* by bilinear interpolation. Therefore, the size of each feature map is $\frac{H}{16} \times \frac{W}{16}$.

Next, we choose useful descriptors that can be converted into items. In [44], a fixed threshold k is used to select top k activations from the full connected layer. However, this may result in the loss of some distinctive activations. In order to avoid this problem, we adopt a more appropriate and flexible strategy. More specifically, we calculate the mean value β of the activation responses larger than 0 as the tunable threshold. A position whose response magnitude is higher than β is highlighted and the index will be converted into an item.

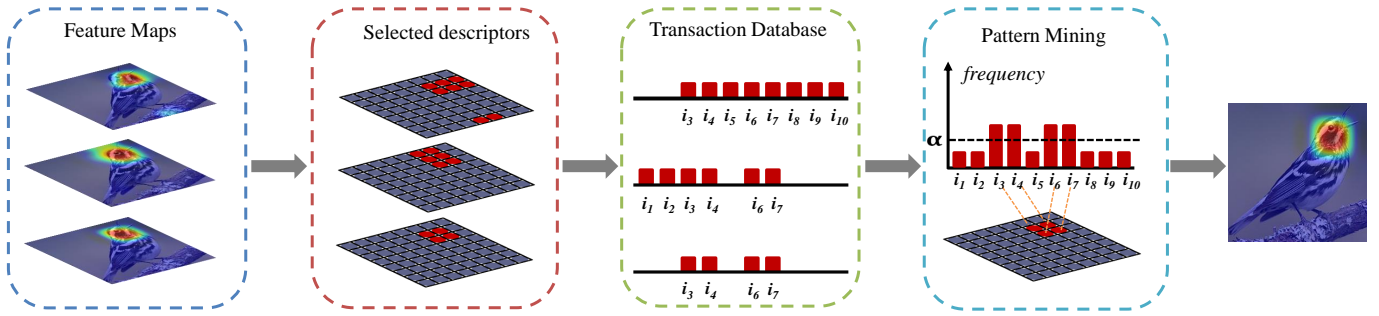


Fig. 4. The detailed process of pattern mining. We first select the descriptors and convert them to items which are utilized to transform the feature maps into a transaction database. $\{i_1, i_2, \dots, i_{10}\}$ is the index set of the highlighted positions, *i.e.* the item set of the transactions. Then we statistically count the frequencies of each item and remain the items whose frequency are greater than α . Finally, we mine the co-occurrence highlighted regions corresponding to the frequent patterns.

As noted in [44], there are two strict requirements for applying pattern mining techniques: 1) only a small number of items can be included in one transaction; 2) only a set of integers can be recorded in one transaction. Fortunately, our proposed transaction conversion satisfies both. First, only small number of regions in each channel are activated. More importantly, the threshold ensures us to select useful descriptors and discard the disturbing descriptors, in particular the activation responses of the background are low, and they will be abandoned. Therefore, it guarantees that the number of activations in each feature map is limited. Second, since we treat the indexes of the selected position in each feature map as items, this ensures that a transaction is recorded with a small set of integers. So our conversion strategy helps us to further mine possible objects successfully using pattern mining techniques.

D. Mining patterns

Given a set of transaction database D , we apply the Apriori algorithm [52] to find the frequent items. For a given minimum support threshold α , an itemset P is considered as frequent if $supp(p) \geq \alpha$. In other words, the support threshold determines which patterns will be mined.

The overall process of pattern mining is shown in Figure 4. First, we convert feature maps to a transaction database using the tunable threshold strategy. Note that the selected positions and the discarded positions are represented by red and blue dots, respectively. Then, we calculate the frequency and keep the items whose frequency is larger than α . For example, we can observe that the frequency of $\{i_3, i_4, i_6, i_7\}$ is greater than α , so we denote these items as a frequent pattern $P = \{i_3, i_4, i_6, i_7\}$. Thus, all frequent patterns are mined and the corresponding regions are discovered.

E. Selecting and Merging the best patterns for object localization

Although patterns are mined in the previous section, some of them may be isolated. Therefore we need to select the optimal patterns for object localization. Here we introduce our selection strategy: *spatial continuity*. In our method, a mined pattern corresponds to a region in one image. Since

one target object is spatially continuous in one image, the object regions represented by selected patterns should also be spatially continuous. In addition, we discover that the isolated regions usually belong to the background of an image. Thus, we attempt to select the largest connected component based on the mined patterns to cover the entire target object as much as possible.

Subsequently, we merge the selected patterns to generate a support map S for each image. Specifically, S is defined as $s(x, y)$, where $s(x, y)$ is the frequency of an item represented by its position (x, y) . Note that the support map S is generated by relevant and non-redundant patterns. The size of support map is same with the feature map. To obtain the support map with the same size as the original image, we upsample the support map by bilinear interpolation. Finally, we take the bounding box that covers the largest connected component in the support map, which is similar to CAM [3]. More significantly, the higher value $s(x, y)$ of the position, the more likely its corresponding region contains a part of a target object.

IV. EXPERIMENTS

In this section, we firstly describe the implementation details and the datasets of the experiments. Then we evaluate OLM on three challenging unsupervised applications: object localization, saliency detection and fine-grained classification.

A. Implementation Details and Datasets

Implementation Details. In our experiments, we extract feature maps from the convolutional layers (*ReLU-5* and *Pool-5*) of the publicly available pre-trained VGG-16 model [17]. Object Mining is implemented with MatConvNet [53].

Datasets: In order to evaluate the performance of the proposed approach, we conduct a set of qualitative and quantitative experiments on eleven benchmark datasets. Specifically CUB-200-2011 [51], Stanford Dog [54], FGVC-Aircrafts [55], Stanford Cars-196 [56], Object Discovery dataset [15], ImageNet Subsets dataset[9] and PASCAL VOC 2007 [57] are used for object localization. In contrast, the other four ones *i.e.* ESSSD [58], PASCAL-S [59], THUR [60], and SOD [40]

are used for saliency detection. Finally we use CUB-200-2011 [51] for fine-grained classification.

- Fine-grained datasets: CUB-200-2011 (200 classes, 11,788 images) [51], Stanford Dogs (120 classes, 20,580 images) [54], Stanford Cars-196 (196 classes, 16,185 images) [56] and FGVC-Aircrafts (100 classes, 10,000 images) [55].
- The Object Discovery Dataset. The Object Discovery dataset [15] contains 15k images in three categories: airplane, car, and horse. To compare with previous co-localization method fairly, we use a subset of the dataset containing 100 images for each category. There are 18, 11, 7 outliers for three categories, respectively.
- The ImageNet Subsets: We follow other co-localization method to chose six subsets of the ImageNet dataset [61]. These subsets are held-out categories from the 1000-label ILSVRC classification. That is to say, these subsets are unseen by pretrained CNN models.
- PASCAL VOC 2007 Dataset: The PASCAL VOC 2007 dataset [57] is one of the most popular datasets for computer vision tasks such as classification, detection, and segmentation, and it contains 5,011 images in 20 object categories. We use all images from train+val datasets to evaluate our method.
- Four salient object benchmark datasets: ECSSD [58] contains 1000 images with multiple objects of different sizes and complex background. The PASCAL-S dataset [59] ascends from the validation set of PASCAL VOC 2010 [62] with 20 object categories and complex scenes. THUR [60] contains 6,233 images about butterfly, coffee mug, dog jump, giraffe, and plane. SOD [40] is a collection of salient object boundaries based on the Berkeley segmentation data set. This data set contains many images with multiple objects making it challenging.

B. Object Localization

Following previous image co-localization works [8], [10], we use the correct localization (CorLoc) to evaluate the proposed method. According the PASCAL-criterion, the CorLoc is defined as: $\frac{area(B_p \cap B_{gt})}{area(B_p \cup B_{gt})} > 0.5$, where B_p is the predicted box and B_{gt} is the ground-truth box.

Fine-Grained datasets.

We conduct experiments on fine-grained datasets following some recently weakly-supervised methods [3], [5], [64] and fully unsupervised method [13]. Table I shows the comparison with the state-of-the-art on four fine-grained datasets. The CorLoc arrives at 80.45%, 80.70%, 94.94% and 92.51% on CUB-200-2011, Stanford Dog, FGVC-Aircrafts and Standford Cars-196, respectively.

Compared with our method, only SCDA [13] is proposed in the same setting. As shown in Table I, we can observe that our method significantly exceeds SCDA on all four datasets (80.45% vs 76.79% on CUB-200-2011, 80.70% vs 78.86% on Dogs, 94.94% vs 94.91% on Aircrafts, 92.51% vs 90.96% on Cars-196). Moreover, our method is only slightly lower than co-localization method [8] (92.51% vs 93.05%) on Cars-196.

Besides, Table I also shows that OLM outperforms recent weakly supervised methods by a large margin. This result

Dataset	Method	Supervision	FullSet
CUB-200-2011	[3]	weakly	59.00*
	[63]	weakly	62.29*
	[5]	weakly	54.08*
	[64]	weakly	56.33*
	[65]	weakly	65.52
	[66]	weakly	56.51
	[8]	co-localization	69.37
	[13]	w/o	76.79
	Ours	w/o	80.45
Stanford Dogs	[66]	weakly	66.68
	[8]	co-localization	36.23
	[13]	w/o	78.86
	Ours	w/o	80.70
FGVC-Aircrafts	[8]	co-localization	42.91
	[13]	w/o	94.91
	Ours	w/o	94.94
Stanford Cars-196	[8]	co-localization	93.05
	[13]	w/o	90.96
	Ours	w/o	92.51

TABLE I
COMPARISONS WITH STATE-OF-THE-ART METHODS ON FOUR FINE-GRAINED DATASETS. NOTE THAT * DENOTES THE TEST SET OF THE FULL CUB-200-2011 DATASET.

Methods	Supervision	Airplane	Car	Horse	Mean
[15]	co-localization	74.39	87.64	63.44	75.16
[6]	co-localization	71.95	93.26	64.52	76.58
[8]	co-localization	82.93	94.38	75.27	84.19
[10]	co-localization	91.46	95.51	77.42	88.13
[13]	fully-unsupervised	87.80	86.52	75.37	83.20
Ours	fully-unsupervised	89.02	89.88	78.49	85.80

TABLE II
COMPARISONS OF CORLOC (%) ON OBJECT DISCOVERY.

may be due to the following reason. Since only image labels can be used in weakly supervised methods, most of them are trained based on classification neural network. Therefore, the generated discriminative areas are only suitable for classification, but may not be optimal for localization. *i.e.* the located areas are small or sparse regions instead of the whole object regions. In contrast, our method is fully unsupervised. We directly reuse the pre-trained model and do not fine-tune on specific dataset, which is beneficial for localizing object regions when incorporating powerful pattern mining techniques. We believe that our work can bring a new insight for solving the localization problem.

The Object Discovery dataset. We further evaluate the performance of our proposed OLM on the Object Discovery dataset. The results are presented in Table II. Note that [15], [6], [10], [8] are co-localization methods, which utilize a set of images containing the objects from the same category.

In Table II, we can observe that OLM approach outperforms unsupervised localization method [13] by 2.6% (85.80% vs 83.20%). Compared with co-localization methods, we also obtain a significant improvement, *i.e.* 1.61% [8], 9.22% [6] and 10.64% [15]. Our method is only lower than [10], which

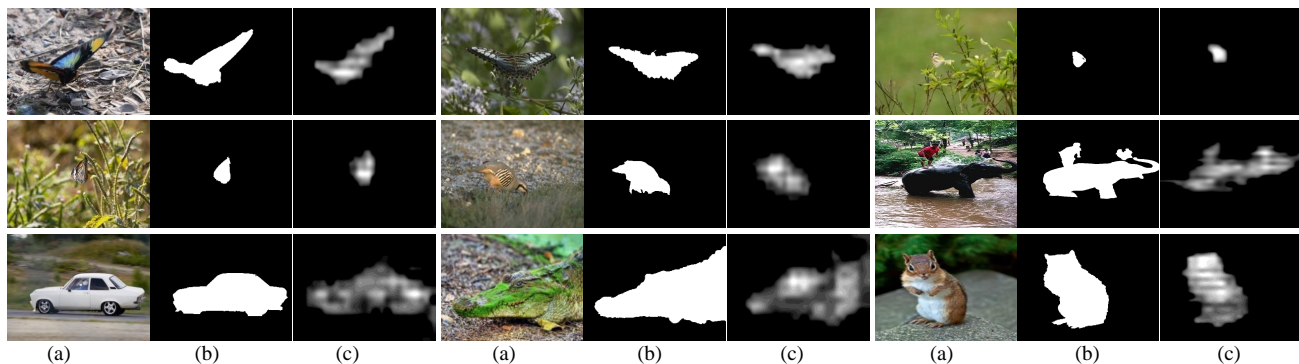


Fig. 6. Examples of the saliency maps. (a) Input images. (b) Ground truth (c)Saliency maps achieved by our method.

Methods	Chipmunk	Rhino	Stoat	Raccoon	Rake	Wheelchair	Mean
[8]	26.6	81.8	44.2	30.1	8.3	35.3	37.7
[9]	44.9	81.8	67.3	41.8	14.5	39.3	48.3
[10]	70.3	93.2	80.8	71.8	30.3	68.2	69.1
[13]	32.3	71.6	52.9	34.0	7.6	28.3	37.8
Ours	67.4	81.7	63.3	56.5	44.9	46.9	60.1

TABLE IV

COMPARISONS OF CORLOC (%) ON IMAGENET SUBSETS. NOTE THAT [8], [9], [10] ARE CO-LOCALIZATION METHODS. ONLY [13] AND OUR METHOD ARE FULLY UNSUPERVISED METHODS.

Methods	ECSSD	PASCAL-S	THUR	SOD
DRFI [40]	.6440	.5745	.5613	.5440
DSR [41]	.6387	.5785	.5498	.5500
MC [39]	.6114	.5742	.5149	.5332
HS [38]	.6234	.5948	.5157	.5383
Ours	.6278	.5827	.5734	.5819

TABLE V

PERFORMANCE OF MEAN F-MEASURE FOR DIFFERENT METHODS INCLUDING OURS ON FOUR BENCHMARK DATASETS.

29.5%). Compared with co-localization method [7], [8], [9], [10], our unsupervised OLM approach also achieve competitive performance, which is only lower than [10] (45.1% vs 46.9%) but higher than any other methods.

Furthermore, in Figure 5(b), we visualize some localization results of our OLM approach on PASCAL VOC 2007. It can be seen that our approach obtains decent object localization results in many challenging scenarios. Specifically, it discovers the precise objects even they are very similar to the background or in a complex background, *e.g.*, the black cat on the tree. More surprisingly, although some images contain multiple objects, OLM can still effectively localize the target objects separately.

ImageNet Subsets dataset. To demonstrate the generalization capabilities of our proposed OLM approach, we follow co-localization methods [8], [9], [10] to conduct experiments on six subsets of the ImageNet. Note that, these subsets are unseen by pretrained CNN models. Table IV presents the CorLoc metric on these subsets.

In Table IV, we can see that OLM outperforms [13] by a large margin (60.1% vs 37.8%) under the unsupervised settings. Compared with co-localization methods, our proposed OLM approach still significantly improves over two co-localization methods by about 22.4% [8] and 11.8% [9] respectively. OLM is only lower than the recent co-localization method [10], but we achieve the best accuracy of 44.9% and outperform [10] by 14.6% on the most difficult category (*i.e.* rake). The competitive results on the challenging ImageNet subsets demonstrate that incorporating pattern mining techniques can efficiently mine target objects in real-world applications in an unsupervised manner.

We visualize some localization results of our OLM approach on the six subsets in Figure 5(c). It can be seen that our approach obtains decent object localization results in many challenging scenarios.

C. Saliency Detection

Although without any annotations, our method can also be used to detect salient regions. We normalize the support map to [0-255] to generate the saliency map. To evaluate the proposed method, we compare our method with state-of-the-art unsupervised saliency methods [40], [39], [41], [38] on four widely used salient object benchmark datasets, including ECSSD [58], PASCAL-S [59], THUR [60], and SOD [40]. We use the F-Measure as evaluation metric, which is defined as

$$F_{\beta} = (1 + \beta^2) \frac{Precision \times Recall}{\beta^2 Precision + Recall}, \quad (2)$$

where adaptive threshold is applied and β^2 is set to 0.3 as suggested in [58], [68].

The comparison is reported in Table V. The THUR dataset is the largest dataset used in this paper, and most of the images have complex background. The result illustrates that our method ranks first on THUR and SOD datasets, which outperforms the state-of-the-art method [41] by 1.21% (57.34% vs 56.13%) and 3.19% (58.19% vs 55%). Our proposed method achieves competitive performance on ECSSD and PASCAL-S. These experiments prove the effectiveness of our proposed pattern mining-based object discovery framework.

Example results of our method are shown in Figure 6, showing that we can achieve satisfactory saliency maps without any annotations.

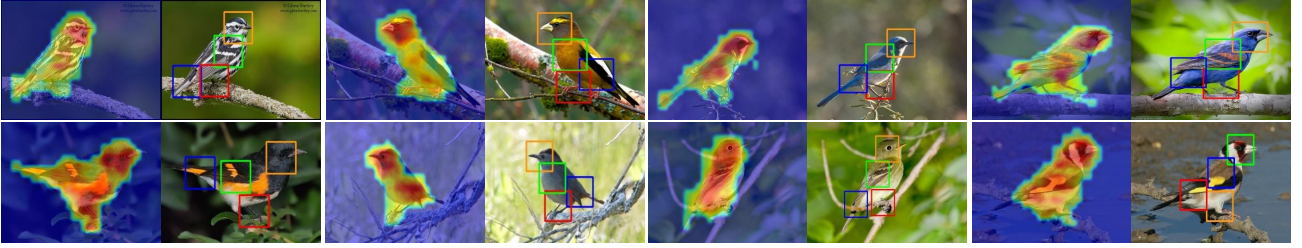


Fig. 7. Examples of the object locations and corresponding part localization results from CUB-200-2011. The yellow, green, blue and red bounding boxes dedicate the head, wing, tail and foot of the bird, respectively. (Best viewed in color)

D. Fine-Grained Classification

Our proposed framework can also be easily applied to fine-grained classification task. Since the subtle visual differences among similar subcategories only locate at the discriminative parts, part localization is a key issue for fine-grained image classification. We observe that some relevant patterns generally correspond to discriminative part regions (e.g. the head of bird) and the part regions are highlighted in the support map. Inspired by this observation, we can divide the regions into several groups of spatial locations. An intuitive idea is to perform the clustering algorithm on those mined patterns.

Specifically, we first produce the clustering data, which are three-dimensional data including the coordinates of each spatial location (x, y) and its corresponding support map value $S(x, y)$. Then we take them as input of the k-means algorithm to cluster these connected regions into K clusters. Surprisingly, the local regions represented by the patterns belonging to one cluster can be regarded as a discriminative part for a fine-grained image. Therefore, we obtain K part locations $\mathbf{C} = \{\mathbf{c}_1, \mathbf{c}_2, \dots, \mathbf{c}_K\}$ in the original image, where $\mathbf{c}_i = (x_i, y_i)$ denotes the coordinates of the i^{th} part.

After getting the part locations, K parts are generated by cropping K squares from \mathbf{I} , with each element of \mathbf{C} as the square center. However, if the side length of the part square is simply fixed, some cropped parts may only include a small part but be disturbed by large background noises. In addition, a fixed-size part may lead to serious overlap with other parts. Therefore, in order to tackle the issues and generate more representative and distinctive parts, we consider a simple and effective geometric constrains to determine the side length l of a part as follows:

$$l = \lambda \times \min\{w_o, h_o\}, \quad (3)$$

where w_o and h_o are width and height of the bounding box generated from the support map, respectively, and λ is a scale factor. Finally, we can define the i^{th} part mask as:

$$\mathbf{M}_i(x, y) = \begin{cases} 1, & \text{if } |x - x_i| \leq \frac{l}{2} \text{ and } |y - y_i| \leq \frac{l}{2} \\ 0, & \text{otherwise} \end{cases}. \quad (4)$$

Thus, the i^{th} part can be computed as follows:

$$\mathbf{I}_i = \mathbf{I} \odot \mathbf{M}_i, \quad (5)$$

where \odot denotes element-wise multiplication.

Figure 7 shows some part localization results by our proposed approach.

Previous works [69], [31] have proved the benefits of joint feature representation, thus we follow the same feature ensemble strategy. We build a multi-stream architecture, composed of *Image stream*, *Object stream* and *Part stream*, with different level images as input. For the classification features of the original image, object and parts, the same CNN model is adopted but fine-tuned on different training data. In our work, we follow [31] to obtain joint part-based representations for each image:

$$\{\mathbf{P}_I, \mathbf{P}_O, \mathbf{P}_1, \mathbf{P}_2, \dots, \mathbf{P}_K\}, \quad (6)$$

where \mathbf{P}_I , \mathbf{P}_O and \mathbf{P}_i denote the feature descriptors of the original image, the object image and the i^{th} part, respectively. We extract the feature maps from the last convolutional layer of *Image stream*, *Object stream* and K *Part stream*, respectively. Then we perform the global average pooling and ℓ_2 -normalization to obtain the above feature descriptors. Finally, we concatenate them to train a classifier for the final classification.

For object/part localization, we use the VGG-16 [17] model pre-trained on ImageNet with 448×448 resolution to extract feature maps from *ReLU-5* and *Pool-5* layers. The minimum support threshold α is set to 0.07. The number of parts K is set to 4. The λ in Equation 3 is empirically set as $\frac{1}{4}$ to produce more representative parts.

Table VI summarizes the classification results on the CUB-200-2011 test set. To make fair comparison, we adopt VGG-16, VGG-19 and ResNet50 as baselines. It is noted that ACoL and ADL are the current state-of-the-art techniques for weakly supervised methods. In contrary, we do not use any annotations to localize object and part regions. In Table VI, we can observe that, using predicted objects annotations, the performance is improved by 2.6% (69.7% vs 72.3%) on VGG-16, 1.9% (75.0% vs 76.9%) on VGG-19 and 0.7% (82.9% vs 83.6%) on ResNet-50. Furthermore, benefited from the localized discriminative parts by our proposed approach, OLM (VGG-19 object+part) and OLM (ResNet-50 object+part) surpass two strong baseline models (VGG-19 on full image and ResNet-50 on full image) by 7.5% and 3.6% significant improvement, respectively. Compared with [63], [5], [3], OLM outperforms them by a noticeable margin. We achieve better classification results than VGGNet-ACoL [5] (82.5% vs 71.90%) and VGGNet-ADL [63] (82.5% vs 65.3%) respectively. OLM (ResNet-50) also achieves the best result among all of the ResNet-50 based methods.

The reason is that our mined regions can locate the dis-

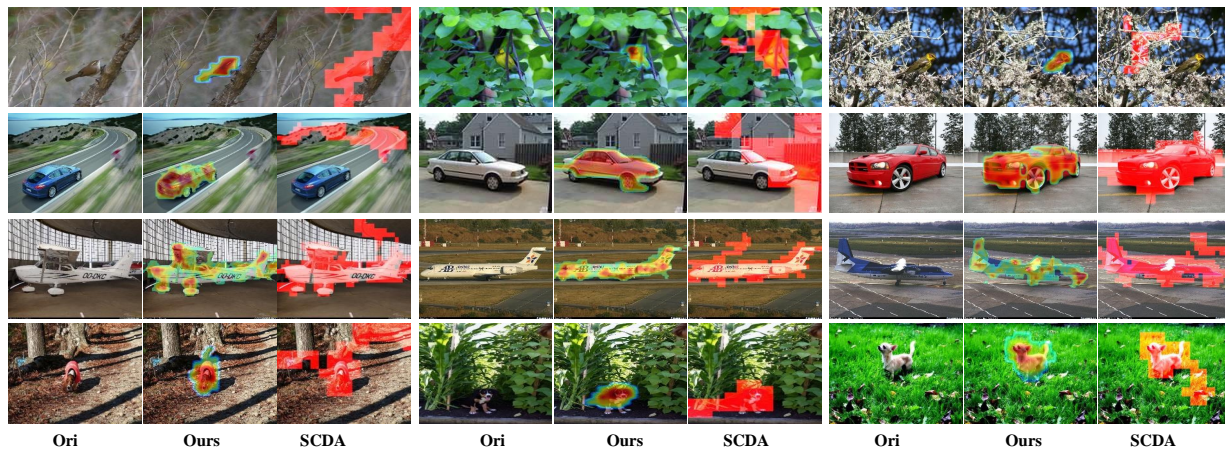


Fig. 8. Comparison with other unsupervised method for generating localization maps. Our method is more robust and can generate more accurate localization maps than SCDA[13] (Best viewed in color.) .

Methods	Acc(%)
GoogLeNet-GAP [3] on full image	63.0
GoogLeNet-GAP [3] with object stream	67.8
GoogLeNet-GAP [3] with BBox	70.5
VGG16 on full image	69.7
VGG19 on full image	75.0
VGGNet-ACoL [5] on full image	71.9
VGGNet-ADL [63] on full image	65.3
VGG16-Ours with object stream	72.3
VGG19-Ours with object stream	76.9
VGG19-Ours with object stream+part stream	82.5
ResNet50 on full image	82.9
ResNet50-GAP [3] on full image	80.6
ResNet50-ADL [63] on full image	80.3
ResNet50-Ours with object stream	83.6
ResNet50-Ours with object stream+part stream	86.2

TABLE VI

CLASSIFICATION RESULTS ON CUB-200-2011, “OBJECT”, AND “PARTS” REPRESENT WHETHER THE METHOD USES THE PREDICT OBJECT ANNOTATIONS, PART ANNOTATIONS.

Methods	Aircrafts	Cars	Dogs	CUB	ImageNet	VOC2007
<i>Mean-threshold</i> [13]	94.9	91.0	78.9	76.8	37.8	29.5
<i>Pattern mining</i>	94.9	92.5	80.7	80.5	60.1	45.1

TABLE VII

QUANTITATIVE RESULTS WITH DIFFERENT STRATEGY.

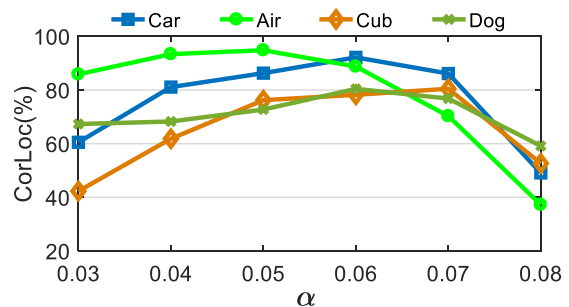


Fig. 9. The localization performances based on different α on four fine-grained datasets.

criminative parts and thus boost the classification performance. Moreover, unlike other techniques [63], [5], [3], our localization approach does not need training process, thus it is very fast to extract objects and parts regions, and can be easily integrated with various classification models.

E. Further Analysis

This section evaluates the effects of the parameter α and the strategy of convolutional feature combination.

The necessity of pattern mining strategy. To verify the localization ability by introducing pattern mining techniques, we give the quantitative and the qualitative comparison with SCDA [13], which also reuses the pre-trained CNN model but employs a simple “mean-threshold” strategy to localize the objects. We detail the impact of our contributions on six datasets: CUB-200-2011, Stanford Dogs, FGVC-aircrafts, Cars-196, VOC 2007 and ImageNet Subsets. The performances are reported in Table VII. We can consistently observe that our pattern mining strategy achieve a significant improvement compared with [13]. The superiority of our approach mainly benefits from introducing the pattern

mining strategy to mine possible object regions. Specially, our approach outperforms [13] by a large gain of 15.6% and 22.3% on two challenging datasets, VOC 2007 and ImageNet subsets, respectively. The results demonstrate that our method is more robust to complex images, which further validates the necessity of using pattern mining techniques. Figure 8 visualizes the localized regions of two methods. It can be seen that our approach obtains decent object localization results in many challenging scenarios. Specifically, in the first rows, our method accurately locate the small objects. More interestingly, it discovers the precise objects even when they are very similar to the background or in a complex background. Meanwhile, our method can localize much finer contour of the objects compared with SCDA.

Impact of parameter α . To investigate the effect of the parameter α on localization performances, we vary α from 0.03 to 0.08, finding that $\alpha = 0.07$, $\alpha = 0.06$, $\alpha = 0.05$, $\alpha = 0.06$ maximizes the accuracy on CUB-200-2011, Stanford Dogs, FGVC-Aircrafts and Stanford Cars-196 respectively, as

Methods	CUB-200-2011	Dogs	Aircrafts	Cars-196
<i>Pool-5</i>	76.64	79.58	93.40	87.30
<i>ReLU-5</i>	65.54	67.33	92.24	84.32
<i>Pool-5&ReLU-5</i>	80.45	80.70	94.94	92.51

TABLE VIII

LOCALIZATION ACCURACY (%) ON FOUR FINE-GRAINED DATASETS WITH DIFFERENT CONVOLUTIONAL LAYERS.

shown in Figure 9. We observe that a well-designed minimum support threshold α improves the performance, and a lower threshold brings background noise while the higher threshold could only discover a small region of a target object.

Strategy of convolutional feature combination. To verify the impact of features extracted from different convolutional layers, we perform the experiment with the following settings. *Pool-5* refers to features maps extracted only with the *Pool-5* layer, and *ReLU-5* represents that features maps extracted only with the *ReLU-5* layer. The localization results using different convolutional layers are reported in Table VIII. Experimental results show that we can achieve significant improvement by combining feature maps extracted from *Pool-5* and *ReLU-5* layers on all four fine-grained datasets. Additionally, we also attempt to combine feature maps from different layers, e.g., *Conv-4*, *Pool-4*. However, the *Conv-4&Pool-4* yields lower accuracy, and the cost of pattern mining method dramatically increases due to the rapid growth of items.

F. Computational complexity

We randomly select 400 images from the *CUB-200-2011* dataset as examples to report the computational complexity. We perform the experiments on a computer with Intel Xeon E5-2683 v3, 128G main memory, and a TITAN Xp GPU. Our proposed OLM approach consists of two major steps: (1) feature extraction and (2) pattern mining-based object localization including transaction creation, pattern mining, and support map generation. The execution time for feature extraction is about 0.03 second/image on GPU and 0.74 second/image on CPU, respectively. The second step only takes about 0.21 second/image on both GPU and CPU. Thus, the execute time is in total about 0.24 second/image on GPU and 0.95 second/image on CPU, respectively. This shows the efficiency of our proposed method in the practical scenario.

V. CONCLUSION

In this paper, we propose a novel pattern mining-based method, called Object Location Mining (OLM), for unsupervised object discovery and localization. Our method exploits the advantage of data mining and feature representation of pre-trained CNN models. The proposed OLM can also be easily extended to the task of saliency detection and fine-grained classification. Experimental results show that OLM achieves competitive performance on a variety of benchmarks, demonstrating the effectiveness of coupling pattern mining with pre-trained model reuse. Our approach does not need any annotations yet still shows promising localization ability, which provides a new perspective to solve the localization problem.

REFERENCES

- [1] W. Liu, D. Anguelov, D. Erhan, C. Szegedy, S. Reed, C. Y. Fu, and A. C. Berg, "Ssd: Single shot multibox detector," in *ECCV*, 2016, pp. 21–37.
- [2] J. Redmon, S. Divvala, R. Girshick, and A. Farhadi, "You only look once: Unified, real-time object detection," in *CVPR*, 2016, pp. 779–788.
- [3] B. Zhou, A. Khosla, A. Lapedriza, A. Oliva, and A. Torralba, "Learning deep features for discriminative localization," in *CVPR*, 2016, pp. 2921–2929.
- [4] T. Durand, T. Mordan, N. Thome, and M. Cord, "Wildcat: Weakly supervised learning of deep convnets for image classification, pointwise localization and segmentation," in *CVPR*, 2017, pp. 5957–5966.
- [5] X. Zhang, Y. Wei, J. Feng, Y. Yang, and T. S. Huang, "Adversarial complementary learning for weakly supervised object localization," in *CVPR*, 2018, pp. 1325–1334.
- [6] K. Tang, A. Joulin, L. J. Li, and F. F. Li, "Co-localization in real-world images," in *CVPR*, 2014, pp. 1464–1471.
- [7] A. Joulin, K. Tang, and F. F. Li, "Efficient image and video co-localization with frank-wolfe algorithm," in *ECCV*, 2014, pp. 253–268.
- [8] M. Cho, S. Kwak, C. Schmid, and J. Ponce, "Unsupervised object discovery and localization in the wild: Part-based matching with bottom-up region proposals," in *CVPR*, 2015, pp. 1201–1210.
- [9] Y. Li, L. Liu, C. Shen, and A. V. D. Hengel, "Image co-localization by mimicking a good detectors confidence score distribution," in *ECCV*, 2016, pp. 19–34.
- [10] X. S. Wei, C. L. Zhang, Y. Li, C. W. Xie, J. Wu, C. Shen, and Z. H. Zhou, "Deep descriptor transforming for image co-localization," in *IJCAI*, 2017, pp. 3048–3054.
- [11] M. D. Zeiler and R. Fergus, "Visualizing and understanding convolutional networks," in *ECCV*, vol. 8689, 2014, pp. 818–833.
- [12] B. Hariharan, P. Arbellez, R. Girshick, and J. Malik, "Hypercolumns for object segmentation and fine-grained localization," in *CVPR*, 2015, pp. 447–456.
- [13] X. S. Wei, J. H. Luo, J. Wu, and Z. H. Zhou, "Selective convolutional descriptor aggregation for fine-grained image retrieval," *IEEE Transactions on Image Processing*, vol. 26, no. 6, pp. 2868–2881, 2017.
- [14] A. Faktor and M. Irani, *Clustering by Composition Unsupervised Discovery of Image Categories*. Springer Berlin Heidelberg, 2012.
- [15] M. Rubinstein, A. Joulin, J. Kopf, and C. Liu, "Unsupervised joint object discovery and segmentation in internet images," in *CVPR*, 2013, pp. 1939–1946.
- [16] B. Zhou, A. Khosla, A. Lapedriza, A. Oliva, and A. Torralba, "Object detectors emerge in deep scene cnns," *Computer Science*, 2015.
- [17] K. Simonyan and A. Zisserman, "Very deep convolutional networks for large-scale image recognition," in *ICLR*, 2014.
- [18] A. Krizhevsky, I. Sutskever, and G. E. Hinton, "Imagenet classification with deep convolutional neural networks," in *NIPS*, 2012, pp. 1097–1105.
- [19] N. Zhang, J. Donahue, R. Girshick, and T. Darrell, "Part-based r-cnns for fine-grained category detection," in *ECCV*. Springer, 2014, pp. 834–849.
- [20] T. Xiao, Y. Xu, K. Yang, J. Zhang, Y. Peng, and Z. Zhang, "The application of two-level attention models in deep convolutional neural network for fine-grained image classification," in *CVPR*, 2015, pp. 842–850.
- [21] T.-Y. Lin, A. RoyChowdhury, and S. Maji, "Bilinear cnn models for fine-grained visual recognition," in *ICCV*, 2015, pp. 1449–1457.
- [22] S. Huang, Z. Xu, D. Tao, and Y. Zhang, "Part-stacked cnn for fine-grained visual categorization," in *CVPR*, 2016, pp. 1173–1182.
- [23] H. Zhang, T. Xu, M. Elhoseiny, X. Huang, S. Zhang, A. Elgammal, and D. Metaxas, "Spda-cnn: Unifying semantic part detection and abstraction for fine-grained recognition," in *CVPR*, 2016, pp. 1143–1152.
- [24] X.-S. Wei, C.-W. Xie, J. Wu, and C. Shen, "Mask-cnn: Localizing parts and selecting descriptors for fine-grained bird species categorization," *Pattern Recognition*, vol. 76, pp. 704–714, 2018.
- [25] Y. Zhang, X.-S. Wei, J. Wu, J. Cai, J. Lu, V.-A. Nguyen, and M. N. Do, "Weakly supervised fine-grained categorization with part-based image representation," *IEEE Transactions on Image Processing*, vol. 25, no. 4, pp. 1713–1725, 2016.
- [26] X. Zhang, H. Xiong, W. Zhou, W. Lin, and Q. Tian, "Picking deep filter responses for fine-grained image recognition," in *CVPR*, 2016, pp. 1134–1142.
- [27] X. He, Y. Peng, and J. Zhao, "Fine-grained discriminative localization via saliency-guided faster r-cnn," in *ACM Multimedia*. ACM, 2017, pp. 627–635.

- [28] B. Zhao, X. Wu, J. Feng, Q. Peng, and S. Yan, "Diversified visual attention networks for fine-grained object classification," *IEEE Transactions on Multimedia*, vol. 19, no. 6, pp. 1245–1256, 2017.
- [29] X. Liu, T. Xia, J. Wang, Y. Yang, F. Zhou, and Y. Lin, "Fully convolutional attention networks for fine-grained recognition," *arXiv*, 2016.
- [30] J. Fu, H. Zheng, and T. Mei, "Look closer to see better: Recurrent attention convolutional neural network for fine-grained image recognition," in *CVPR*, 2017, pp. 4438–4446.
- [31] H. Zheng, J. Fu, T. Mei, and J. Luo, "Learning multi-attention convolutional neural network for fine-grained image recognition," in *ICCV*, 2017, pp. 5209–5217.
- [32] L. Zhang, Y. Yang, M. Wang, R. Hong, L. Nie, and X. Li, "Detecting densely distributed graph patterns for fine-grained image categorization," *IEEE Transactions on Image Processing*, vol. 25, no. 2, pp. 553–565, 2016.
- [33] J. R. Uijlings, K. E. Van De Sande, T. Gevers, and A. W. Smeulders, "Selective search for object recognition," *ICCV*, vol. 104, no. 2, pp. 154–171, 2013.
- [34] P. Sermanet, A. Frome, and E. Real, "Attention for fine-grained categorization," 2014.
- [35] M. Simon and E. Rodner, "Neural activation constellations: Unsupervised part model discovery with convolutional networks," in *ICCV*, 2015, pp. 1143–1151.
- [36] A. Borji, M.-M. Cheng, H. Jiang, and J. Li, "Salient object detection: A survey," *ArXiv e-prints*, 2014.
- [37] W. Wang, Q. Lai, H. Fu, J. Shen, and H. Ling, "Salient object detection in the deep learning era: An in-depth survey," 2019. [Online]. Available: <http://arxiv.org/abs/1904.09146>
- [38] W. Zou and N. Komodakis, "Harf: Hierarchy-associated rich features for salient object detection," in *ICCV*, 2015.
- [39] B. Jiang, L. Zhang, H. Lu, C. Yang, and M. H. Yang, "Saliency detection via absorbing markov chain," in *ICCV*, 2013.
- [40] H. Jiang, J. Wang, Z. Yuan, W. Yang, N. Zheng, and S. Li, "Salient object detection: A discriminative regional feature integration approach," in *CVPR*, 2013.
- [41] X. Li, H. Lu, L. Zhang, R. Xiang, and M. H. Yang, "Saliency detection via dense and sparse reconstruction," in *ICCV*, 2013.
- [42] D. Zhang, J. Han, and Z. Yu, "Supervision by fusion: Towards unsupervised learning of deep salient object detector," in *ICCV*, 2017.
- [43] J. Zhang, T. Zhang, Y. Dai, M. Harandi, and R. Hartley, "Deep unsupervised saliency detection: A multiple noisy labeling perspective," in *CVPR*, June 2018.
- [44] Y. Li, L. Liu, C. Shen, and A. V. D. Hengel, "Mining mid-level visual patterns with deep cnn activations," *IJCV*, vol. 121, no. 3, pp. 1–21, 2016.
- [45] B. Fernando and T. Tuytelaars, "Mining multiple queries for image retrieval: On-the-fly learning of an object-specific mid-level representation," in *ICCV*, 2014, pp. 2544–2551.
- [46] K. Rematas, B. Fernando, F. Dellaert, and T. Tuytelaars, "Dataset fingerprints: Exploring image collections through data mining," in *CVPR*, 2015, pp. 4867–4875.
- [47] T. Quack, V. Ferrari, B. Leibe, and L. J. V. Gool, "Efficient mining of frequent and distinctive feature configurations," in *ICCV*, 2007, pp. 1–8.
- [48] J. Yuan, Y. Wu, and M. Yang, "Discovery of collocation patterns: from visual words to visual phrases," in *CVPR*, 2007, pp. 1–8.
- [49] A. Agarwal and B. Triggs, "Multilevel image coding with hyperfeatures," *IJCV*, vol. 78, no. 1, pp. 15–27, 2008.
- [50] B. Fernando, E. Fromont, and T. Tuytelaars, "Mining mid-level features for image classification," *IJCV*, vol. 108, no. 3, pp. 186–203, 2014.
- [51] C. Wah, S. Branson, P. Welinder, P. Perona, and S. Belongie, "The caltech-ucsd birds200-2011 dataset," *California Institute of Technology*, 2011.
- [52] R. Agrawal and R. Srikant, "Fast algorithms for mining association rules in large databases," in *VLDB*, 1994, pp. 487–499.
- [53] A. Vedaldi and K. Lenc, "Matconvnet: Convolutional neural networks for matlab," in *ACM Multimedia*, 2015, pp. 689–692.
- [54] A. Khosla, N. Jayadevaprakash, B. Yao, and F. fei Li, "L.: Novel dataset for fine-grained image categorization," in *CVPR Workshop on FGVC*, 2011.
- [55] S. Maji, E. Rahtu, J. Kannala, M. Blaschko, and A. Vedaldi, "Fine-grained visual classification of aircraft," *HAL-INRIA*, 2013.
- [56] J. Krause, M. Stark, D. Jia, and F. F. Li, "3d object representations for fine-grained categorization," in *ICCV Workshops*, 2013, pp. 554–561.
- [57] M. Everingham, L. Van Gool, C. K. I. Williams, J. Winn, and A. Zisserman, "The PASCAL Visual Object Classes Challenge 2007 (VOC2007) Results."
- [58] Q. Yan, X. Li, J. Shi, and J. Jia, "Hierarchical saliency detection," 2013.
- [59] L. Yin, X. Hou, C. Koch, J. M. Rehg, and A. L. Yuille, "The secrets of salient object segmentation," in *CVPR*, 2014.
- [60] M.-M. Cheng, N. Mitra, X. Huang, and S.-M. Hu, "Salientshape: group saliency in image collections," *The Visual Computer*, vol. 30, no. 4, pp. 443–453, 2014.
- [61] J. Deng, W. Dong, R. Socher, L. Li, K. Li, and L. Fei-Fei, "Imagenet: A large-scale hierarchical image database," in *CVPR*, 2009, pp. 248–255.
- [62] M. Everingham, L. Van Gool, C. K. I. Williams, J. Winn, and A. Zisserman, "The pascal visual object classes (voc) challenge," *IJCV*, vol. 88, no. 2, pp. 303–338, June 2010.
- [63] J. Choe and H. Shim, "Attention-based dropout layer for weakly supervised object localization," in *CVPR*, June 2019.
- [64] X. Zhang, Y. Wei, G. Kang, Y. Yang, and T. S. Huang, "Self-produced guidance for weakly-supervised object localization," in *ECCV*, 2018.
- [65] X. He and Y. Peng, "Weakly supervised learning of part selection model with spatial constraints for fine-grained image classification," in *AAAI*, 2017, pp. 4075–4081.
- [66] Z. Xu, D. Tao, S. Huang, and Y. Zhang, "Friend or foe: Fine-grained categorization with weak supervision," *IEEE Transactions on Image Processing*, vol. 26, no. 1, pp. 135–146, 2017.
- [67] C. Wang, W. Ren, K. Huang, and T. Tan, "Weakly supervised object localization with latent category learning," in *ECCV*, 2014, pp. 431–445.
- [68] R. Achanta, S. Hemamiz, F. Estraday, and S. Ssstrunky, "Frequency-tuned salient region detection," in *CVPR*, 2009.
- [69] Y. Peng, X. He, and J. Zhao, "Object-part attention model for fine-grained image classification," *IEEE Transactions on Image Processing*, vol. 27, no. 3, pp. 1487–1500, 2018.